Adsorption Kinetics of Polystyrene onto Germanium from a Carbon Tetrachloride Solution

Alexander Couzis† and Erdogan Gulari*

Department of Chemical Engineering, The University of Michigan, Ann Arbor, Michigan 48109

Received July 15, 1993; Revised Manuscript Received February 22, 1994®

ABSTRACT: We report the results of an experimental study of adsorption as a function of concentration and molecular weight for the system *polystyrene/carbon tetrachloride/germanium*. Adsorption measurements were made using Fourier transform infrared attenuated total reflection spectroscopy (FTIR-ATR). We find a strong dependence of adsorption on the bulk solution concentration and the molecular weight of the adsorbing polymer. The data provide evidence that the rate limiting step for the adsorption process is the entry of new macromolecular chains into the immediately formed and highly constrained polymer layer. A theoretical model based on the scaling concepts, first introduced by de Gennes, is proposed, and its predictions are compared with the experimental data. The data also suggest the presence of a highly constrained (glassylike) layer, with a structure that depends on the parameters of the system.

Introduction

Adsorption of macromolecules at interfaces (solid–liquid, liquid–gas, or liquid–liquid) plays a vital role in a variety of industrial, technological, and biological applications. Adhesion, flocculation, and stabilization of colloid particles, chromatography (column technology), reinforcement of brittle materials, artificial organs in medicine, interconnect devices, and microelectronics packaging and processing are a few examples of these applications.

The focal point of this paper is to present a study of the adsorption kinetics of a homopolymer onto a solid surface that is in contact with a solution of the polymer. Equilibrium studies of such systems have been reported extensively.[1–3] In comparison, kinetic studies have been sparse, leading to very little information on the mechanisms involved. Thus, the dynamics of polymer adsorption is a largely unsolved problem which has attracted attention only recently.

Different experimental techniques have been used for studying the process of polymer adsorption onto the solid–liquid interface. Ellipsometry[4–7] has been used to measure the thickness of the adsorbed polymer, and the adsorbed amount in equilibrium. In these studies the molecular weight and solution concentration effects are discussed, but the range of concentration is limited to the dilute regime. Hydrodynamic methods[8,9] and neutron scattering[10,11] have been used to study the conformations of the adsorbed polymers on the solid–liquid interface. Measurements using infrared spectroscopy,[12,13] of the fraction of surface sites occupied by the polymer and the fraction of polymer segments in trains have given insight on the conformations of the polymers on the interface as well. In almost all of the above mentioned studies equilibrium measurements were made. It was not until recently that studies of the dynamics of polymer adsorption have appeared, using a variety of techniques. Radioactive tracing[14–17] of ^{3}H labeled polymers has been used to monitor the rates of exchange of flexible polymers at the solid–liquid interface. Ellipsometry is also used for studying long time scale kinetics, but its application is limited to systems where the difference in the refractive index between the solution and the adsorbed film is substantial. Surface plasma oscillations[18,19] have been used to study the adsorption of polystyrene and block copolymers onto silver surfaces. Finally, attenuated total reflection (ATR) spectroscopy[20–25] has been used to study the adsorption of a number of polymers on semiconductor surfaces such as germanium and silicon.

Table 1. Characteristics of the Polystyrenes Used in This Study

type	mol wt	M_w/M_n
#16239	600 000	1.10
F-380	3 840 000	1.05
F-850	8 420 000	1.17
F-2000	20 600 000	

In this work, *in situ* measurements of the adsorption kinetics of polystyrene onto germanium from a carbon tetrachloride solution are presented. The effects of molecular weight and solution concentration are discussed. An extension to the kinetic model first presented by de Gennes[26,27] describing the entry and spreading processes involved is proposed and compared to the experimental results. The validity of the model is verified by the correct prediction of the microscopic jump time, characteristic of the polymer and the environment in which it resides. We believe this study to be the first to report adsorption data for samples with a large degree of polymerization at concentrations above the entanglement concentration. For the first time a model describing the reptation processes involved in the adsorbed layer is directly compared to experimental data and shown to work rather well. Indirect evidence of the initially constrained layer is also presented.

Experimental Details

Materials. Linear polystyrene, with a narrow molecular weight distribution, was purchased from Toyo Soda Manufacturing Co. The 600 000 molecular weight sample was purchased from Polysciences, Inc. The specifications of the samples used are given in Table 1. HPLC grade carbon tetrachloride was purchased from Aldrich Chemicals and was used without further purification. The substrate used was the attenuated reflection element itself. The elements used were germanium ATR elements purchased from Harrick Scientific Co. with dimensions 50 × 10 × 3 mm and angle of incidence of 45°.

Experimental Technique. The kinetics of adsorption of polystyrene molecules onto the germanium surface have been monitored with Fourier transform infrared spectroscopy with an

* To whom correspondance should be addressed.
† International Paper Co., Long Meadow Rd., Tuxedo, NY 10924.
® Abstract published in *Advance ACS Abstracts*, May 15, 1994.

0024-9297/94/2227-3580$04.50/0

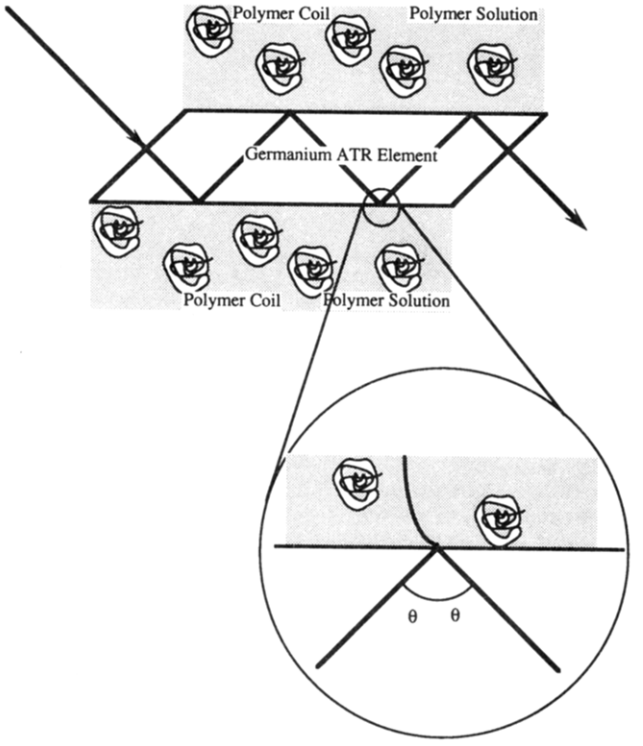

Figure 1. Attenuated total reflection geometry used for the *in situ* measurement of the polymer's adsorbed amount.

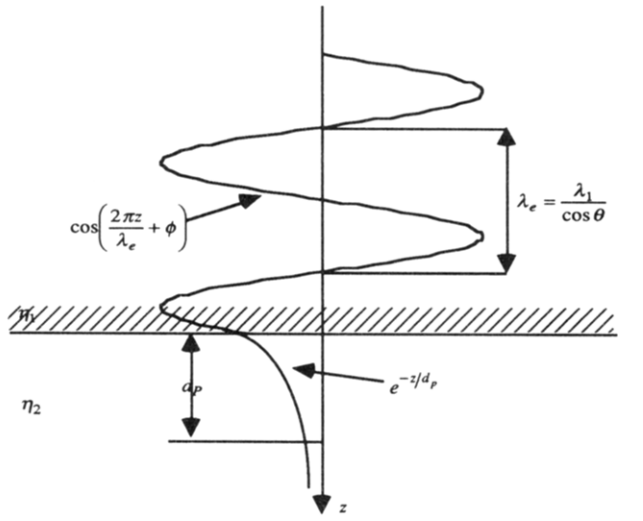

Figure 2. Standing wave amplitudes established at a totally reflecting interface.

attenuated total internal reflection liquid cell (FTIR-ATR). A schematic description of the technique can be seen in Figure 1.

Total internal reflection is a familiar phenomenon, observed in everyday life. When a light beam propagating in an optical medium with a refractive index of η_1, strikes a surface of another material, with a refractive index η_2, a portion of the beam will be reflected and a portion will be partially transmitted in the second medium. When the light approaches the interface from a denser medium ($\eta_1 > \eta_2$) and the angle of incidence is greater than the critical angle defined by eq 1:

$$\theta > \theta_{\text{critical}} = \arcsin\left(\frac{\eta_2}{\eta_1}\right) \tag{1}$$

total reflection takes place; i.e., there is no transmitted portion of the incident beam. When total reflection takes place at an interface a standing wave is established near the interface, on the denser medium side. In the rarer medium an evanescent wave that has an exponentially decreasing amplitude is created:

$$E = E_0 e^{-z/d_p} \tag{2}$$

The interaction of the evanescent wave with the adsorbing rarer medium causes a loss of reflection. The stronger the interaction, the greater the loss of reflectivity. Reflectivity is defined as the ratio of the reflected light intensity, I, to the intensity of the incident light, I_0:

$$R = \frac{I}{I_0} \tag{3}$$

For small absorption losses (<10%), the strength of interaction can be expressed in terms of an effective thickness, d_e, in a manner similar to the path length used in transmission spectroscopy:

$$R = \frac{I}{I_0} = e^{-\alpha d_e} \underset{\alpha d_e < 0.1}{\rightarrow} R = \frac{I}{I_0} \approx 1 - \alpha d_e \tag{4}$$

In order to calculate the effective thickness we use the bulk material approximation, that is we assume that the rarer medium is much thicker than the penetration depth of the evanascent wave. With this assumption the absorbance per reflection is given by[28]

$$\frac{A}{N_r} = \frac{1}{\cos\theta}\int_0^\infty \alpha E^2\, dz \overset{[3.3]}{\rightarrow} \frac{A}{N_r} = \frac{E_0^{\,2}}{\cos\theta}\int_0^\infty \alpha e^{-2z/d_p}\, dz \tag{5}$$

The above equation has been developed independently by a number of investigators.[29-32] The absorption coefficient contains the effect of both concentration and molecular identity, $\alpha = C\epsilon$, and thus substituting into eq 5 gives us eq 6 which relates quantities that are measured to quantities of interest:

$$\frac{A}{N_r} = \frac{E_0^{\,2}}{\cos\theta}\epsilon\int_0^\infty C(z)e^{-2z/d_p}\, dz \tag{6}$$

From eq 6 we can then calculate the surface excess of an adsorbing molecule.[33-36] To do so we define the following concentration profile:

$$C(z) = \begin{cases} C_b + C_i & \text{for } 0 < z < l \\ C_b & \text{for } l < z < \infty \end{cases} \tag{7}$$

Substituting into eq 7 and integrating result in an equation that relates the total absorption measured to the bulk solution concentration and the surface excess, $\Gamma_i = C_{il}$.

$$\frac{A_{\text{total}}}{N_r} = \epsilon C_b d_e + \epsilon\left(\frac{2d_e}{d_p}\right)(C_{il}) \tag{8}$$

Equation 8 has been used throughout this study for calculating the surface excess of adsorbing polymers at the solid-liquid interface. The molecular extinction coefficient ϵ needed in the above equation is calculated from transmission experiments.

In our studies the effective sampling depth was 1.16 μm at 700 wavenumbers (λ = 14.33 μm) for a 45° angle of incidence.

Experimental Procedure. Solutions of four different concentrations were prepared for MW 3 840 000, and the "apparent" diffusion coefficients were measured by quasielastic light scattering. The equivalent sphere hydrodynamic radii were calculated from the Stokes-Einstein relationship. The results can be seen in Table 2. The radius of gyration of the polymer was determined to be 600 Å. From this data we calculated the entanglement concentration, C^*, to be 0.007 g/mL. Before each experiment a thorough cleaning procedure of the ATR element was followed. At first, the element was mildly polished using a 0.3-μm Al_2O_3 powder, followed by rinsing with acetone, water, and carbon tetrachloride in succession. The rinsing procedure was repeated twice. The Teflon blocks used in the ATR holder were sonicated in a detergent solution for 6 h, then rinsed with water and acetone, and dried. The success of the cleaning procedure was determined by taking the spectra of the cell with and without carbon tetrachloride. If any peak that could not be recognized or did not correspond to a clean system was found,

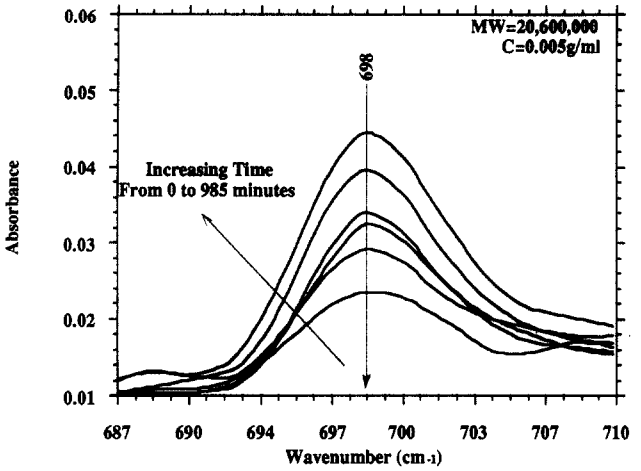

Figure 3. Typical series of spectra of the adsorbing polystyrene on germanium from the carbon tetrachloride solution. The molecular weight of the adsorbing polymer is 20 600 000, and the solution concentration is 0.5 g/mL.

Table 2. Apparent Diffusion Coefficients and Calculated Equivalent Sphere Hydrodynamic (Using the Stokes–Einstein Relationship) Radii as a Function of Concentration for MW = 3 840 000 Polystyrene in CCl_4

concn (g/mL)	diffusion coeff (cm^2/s)	hydrodynamic radius (Å)
0.002	7.14×10^{-8}	667
0.004	8.68×10^{-8}	549
0.006	1.15×10^{-7}	413
0.008	1.11×10^{-7}	428

the cleaning procedure was repeated. This strict cleaning procedure ensured that we had a surface and cell free of impurities or of a level beyond the sensitivity of the IR spectrometer.

The adsorption of the polymer was monitored by the increase in the integrated area of the IR band at 698 cm^{-1}. This absorption band corresponds to the out of plane vibration of the aromatic C–H bond.[37,38] Spectra of the germanium element in contact with the polystyrene solution were taken over a time period ranging from 50 to 60 h, with a time resolution of 3–30 min and wavelength resolution of 4 cm^{-1}. The spectrum of the clean cell was used for the background. Every spectrum was the average of 200 interferograms. All measurements were made with a Mattson Cygnus-100 FT-IR, using a wide band MCT detector. A time series of spectra of the 698-cm^{-1} band can be seen in Figure 3. While the peak absorbance of the band monitored is only about 0.05, the signal to noise ratio at this point is at least 2 orders of magnitude better than the noise. Integration of the total peak area improves the signal to noise ratio even further. The experimental measurements carried out at different times with different crystals and polymer samples were reproducible to ±15% of the adsorbed amount calculated.

Experimental Results

Figure 4 shows the surface excess of polystyrene at the germanium–solution interface as a function of time and solution concentration for the 3 840 000 molecular weight sample. The concentration of the polymer in the bulk solution appears to have a very significant effect on the kinetics of the adsorption of the polystyrene onto the germanium surface: (i) the initial rate of adsorption increases with concentration, (ii) the time needed to attain a constant surface excess decreases as the concentration increases.

For the two lowest concentrations (0.002 and 0.004 g/mL) a near-linear increase in the surface excess with time is observed. When the adsorbed amount is plotted against the square root of time, as shown in Figure 5, a linear behavior is observed for the initial 100 000 s. A diffusion coefficient can then be calculated from the penetration equation:

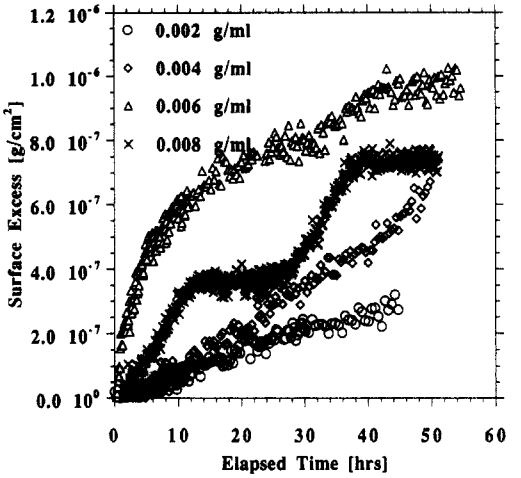

Figure 4. Surface excess of adsorbed polystyrene as a function of time and solution concentration. The molecular weight of the adsorbing polymer is 3 840 000.

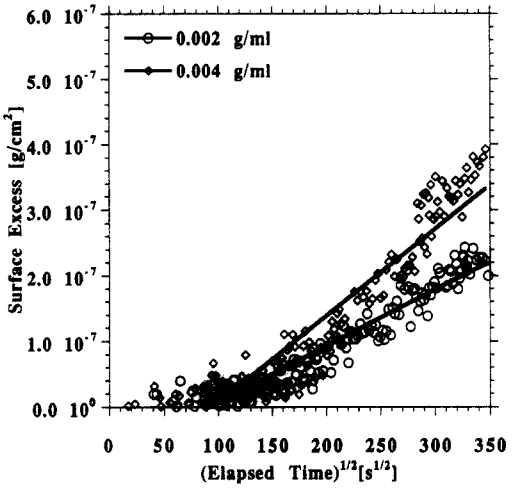

Figure 5. Surface excess of adsorbed polystyrene as a function of the square root of time and solution concentration. The molecular weight of the adsorbing polymer is 3 840 000.

$$\Gamma_i = 2c\sqrt{Dt/\pi} \tag{9}$$

The values obtained for D are 5×10^{-14} and 2×10^{-14} cm^2/s, respectively, for the two samples. These values are 6 orders of magnitude smaller than the diffusion coefficient values obtained from the light scattering experiments for the diffusion of the polymer in solution. However, these values are in the range of tracer diffusion coefficients of polystyrene in dense networks via reptation.[27] This indicates that the process is not controlled by the diffusion of the polymer chains to the interface through a stagnant boundary layer. Instead, as will be shown in the following sections, the data suggest that the rate of adsorption is limited by the barrier encountered by the incoming polymer because of the layer of constrained chains that is formed immediately upon contact of the solution and the solid interface. The slope of the adsorption curve for the 0.004 g/mL solution is higher than that for the 0.002 g/mL solution. For these concentrations total equilibrium is not reached even after 50 h.

For the 0.006 g/mL solution, which is below the entanglement concentration, the shape of the kinetic curve for adsorption changes considerably. The surface excess shows an initial steep rise followed by a constant decrease in the rate of adsorption, leading to an almost constant amount adsorbed after approximately 42 h. The overall shape of the adsorption curve with time resembles that of

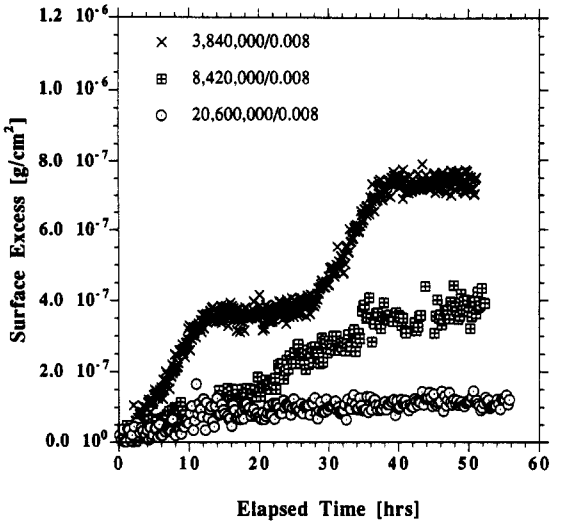

Figure 6. Surface excess of adsorbed polystyrene as a function of time and molecular weight. The solution concentration is 0.008 g/mL.

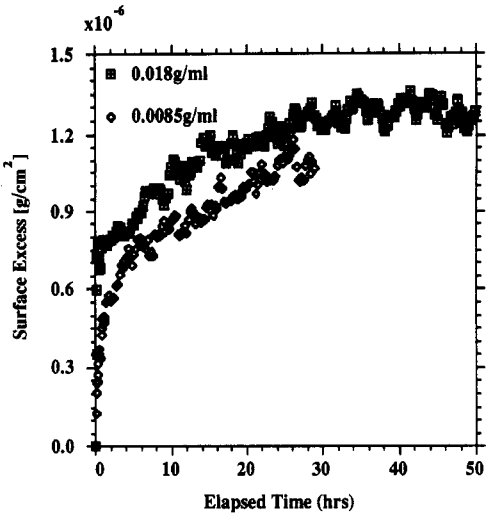

Figure 7. Surface excess of adsorbed polystyrene (MW = 600 000) as a function of time and concentration.

a process exhibiting first order kinetics. The adsorbed amount for this sample is greater at all times compared to the lower concentration solutions. This indicates that the fraction of monomers per polymer chain adsorbed on the solid surface is less than that of the more dilute solutions. In return this would suggest that the adsorbed layer is more fluidlike, thus offering less resistance to the incoming polymer chains.

For the 0.008 g/mL sample the shape of the adsorption curve is very unusual. Initially, the surface excess rises quickly and after 10 h reaches a constant value. Between 10 and 25 h, the adsorbed amount does not increase. After the 15-h induction period and adsorption resumes again and reaches a new constant value after 40 h. The initial rate of adsorption for the 0.008 g/mL sample is less than that of the 0.006 g/mL sample as well. Because of the unusual behavior of this sample, we speculate that several processes are taking place simultaneously, which are discussed in detail in the following section.

Figure 6 shows the surface excess as a function of molecular weight and time at a constant bulk concentration of 0.008 g/mL (in the entanglement regime for all three samples). We again see significant differences in the shape of adsorption curves. The data for the 3 840 000 molecular weight sample show the distinct plateaus discussed earlier. The data for the sample with molecular weight of 8 420 000 exhibit a slow and near-linear increase with time. For this sample no constant value of the adsorbed amount is reached even after 50 h. In contrast, the data for the 20 600 000 molecular weight sample exhibit a very small increase of the adsorbed amount, approximately 30%, during the first 15 h and then the adsorbed amount remains constant within experimental accuracy.

The absolute amounts of the surface excess are also significantly different. After 50 h the 3 840 000 sample when compared to the 8 420 000 and 20 600 000 samples exhibits a surface excess larger by 2.25 and 9 times respectively. This observation is in contrast with previous experimental reports that have shown that the adsorbed amount at equilibrium increases with molecular weight. The significant difference in this study is that even after 50 h of contact of the solution with the solid surface, equilibrium is not established. This is primarily due to the very high molecular weight of the polymers used. The majority of the previous studies were done with polymers smaller by 1 order of magnitude. A result similar to ours was observed by Grannick and his co-workers. They have suggested the presence of nonequilibrium states that are very long lived.[21] Figure 7 shows the surface excess of polystyrene with a molecular weight of 600 000 as a function of two concentrations. The more concentrated sample is at the entanglement concentration, 0.018 g/mL. The dilute solution is half the previous solution's concentration. The surface excess for the concentrated solution exhibits a very steep initial rise, reaching an intermediate saturation point within 1 h from the initial contact of the solution and the germanium. The amount adsorbed remains relatively constant for 4 h and then increases again. The rate of increase in this section is much less than the initial rate. Finally, the adsorbed amount reaches a final value of 1.4×10^{-6} g/cm^2 within approximately 28 h. The lower concentration sample of the same molecular weight exhibits a monotonic increase of the adsorbed amount, with a smaller initial rate. The adsorbed amount does not reach a constant value even after 28 h of contact of the solution and the solid surface. The adsorbed amounts measured for this molecular weight are larger than the amounts measured for any of the other higher molecular weights. This observation is in agreement with the trend discussed for the samples of 0.008 g/mL concentration. The initial higher rate for the concentrated sample is also expected, because the initial process of adsorption is diffusion of the adsorbing material to the surface, which will be favored by higher solution concentrations.

Theoretical Analysis

Equilibrium Structure of the Adsorbed Layer. As already discussed, the majority of the theoretical studies on adsorption of polymers onto a liquid–solid interface have focused on the equilibrium properties of the adsorbed layers. This effort, along with a variety of experiments have shown that at equilibrium the adsorbed layer adopts a self-similar structure.[39] A structure is defined to be self-similar if the mesh size, ζ, at a particular distance from the interface is equal to that distance:

$$\xi(\phi(z)) = z \tag{10}$$

Following (19) it can then be shown that

$$\phi(z) = (\alpha/z)^{4/3} \tag{11}$$

The maximum thickness of the layer is equal to the size of one polymer coil in bulk solution, $z_{max} = R_F = \alpha N^{3/5}$.

Reptation of Polymers. The concentrated nature of the adsorbed polymer layer makes it necessary to introduce the mechanism of motion of the macromolecular chains in such an environment. A polymer in solution adopts a geometry known as the random coil configuration. The size of this configuration, described by the radius of gyration, $\langle s^2\rangle_0^{1/2}$, is proportional to the square root of the molecular weight of the polymer. When the concentration of the polymer in the solution exceeds a critical entanglement concentration, given by

$$c^* = \frac{N}{^4/_3\pi R_F{}^3 N_A 12} \tag{12}$$

the coils begin to overlap. In this concentration regime the polymer chains begin to move from one large scale conformation to another primarily by reptation, a process that resembles diffusion in a snakelike fashion. These types of conformational changes depend on the large scale chain motion, which is a very slow process.

The notion of reptation was first introduced by de Gennes[40] for diffusion of unattached chains in a permanent network and was later extended to independently moving chains by Doi and Edwards.[41] The main point from the latter theory is that the conformational lifetime varies as N^3:

$$\tau_t = \tau_0 N^3 \tag{13}$$

Thus, the diffusion coefficient for reptation is inversely proportional to the molecular weight of the polymer. The macroscopic diffusion coefficient, governing the motion of the center of gravity of the chain, is inversely proportional to the square of the molecular weight of the chain.

Hydrodynamic Friction of Macromolecules in Solution. When a particle moves relative to a fluid surrounding it, the concomitant viscous forces exert a drag on the particle. Similarly, when a polymer moves within a solvent, a drag force is exerted upon the polymer and its monomeric building units. These forces are calculated by solving the Navier–Stokes equation that pertains to the geometry and conditions of the random coil. Such a process is very elaborate; thus for simplification reasons the polymer is represented by the *pear necklace* model. In this model each monomeric unit is considered to behave as a small sphere of radius a. Following the procedures described by Kirkwood,[42] and assuming a very large degree of polymerization ($N \to \infty$), one can show that the friction coefficient, ξ_s, of a collection of N beads is

$$\zeta_s N = 6\pi\nu\langle s^2\rangle_0{}^{1/2}\frac{3}{8}\sqrt{\pi} \tag{14}$$

For the present study carbon tetrachloride is a good solvent for polystyrene, and thus the solution viscosity can be evaluated from[40]

$$\nu = \nu_s\left[1 + 2.5\frac{c}{N}\frac{4\pi}{3}R_h{}^3\right] \tag{15}$$

From the monomeric friction coefficient, ζ_s, we can then calculate the microscopic jump time, τ_0 of a monomer unit, which can be thought of as the time needed for the monomer unit to propagate one step of its random walk motion:

$$\tau_0 = \frac{\zeta_s a^2}{kT} \tag{16}$$

Typical values of the microscopic jump time are in the picosecond range.

Mechanism of Adsorption. Previous theoretical work[26,27,43] has established that the adsorption of polymers onto a solid surface that is in contact with the polymer's solution involves four successive processes: (i) diffusion of the polymer to the solid surface through a stagnant boundary layer; (ii) initial adsorptin in a flat configuration that results in a glassylike layer, if the glass transition temperature of the adsorbing polymer is equal to or above room temperature;[44,45] (iii) entry of additional polymer molecules into the established layer; (iv) spreading of the new polymers in order to reach equilibrium configuration.

The first two stages described above are relatively fast and cannot be monitored experimentally with the technique we have employed. These two processes are relatively easy to model, and a detailed model has been proposed by de Gennes.[27] The time resolution achieved by the experimental technique used, described in the previous sections, allows us to monitor the remaining two stages, which are significantly slower. In the following analysis both entry and spreading are considered as reptation processes.

The amount of polymer adsorbed by a solid surface can be described in many different ways. In the following analysis, the starvation coefficient, x, shall be used, as defined by de Gennes:[27]

$$\Gamma = \Gamma_0(1 - x) \tag{17}$$

Entry versus Spreading. During entry the polymer chain has no direct contact with the solid surface; the friction encountered by the macromolecular chain is primarily due to the weak monomer–solvent friction, ζ_s, described in the previous section. For monomers that are very close to the solid surface the barrier encountered is much stronger because of the glassy features of the first adsorbed layer. In this case, the monomeric friction coefficient, ζ_G, equals

$$\zeta_G = f\zeta_s \quad \text{with } f \gg 1 \tag{18}$$

The dimensionless factor f is a measure of the special frictions encountered in the first glassy layer.

The barrier encountered by the entering polymer resembles a quantum mechanical tunneling barrier and it is described by a transmission coefficient, ϑ. For a saturated polymer layer, ϑ depends only on the molecular weight of the adsorbed polymer. For starved adsorbed layers the transmission coefficient depends on the degree of starvation of the layer.

$$\vartheta = \begin{cases} N^{-0.3} & \text{(saturated layer)} \\ x^{3/2} & \text{(starved layer)} \end{cases} \tag{19}$$

From the above we are led to an entry time:

$$\tau_e = \tau_0 N^3 \vartheta^{-1} \tag{20}$$

For the spreading process the friction is dominated by the wall and by the presence of a glassy layer very close to the wall. The monomer friction coefficient is then given by eq 16. de Gennes has shown that when the thickness of the adsorbed layer, l, is less than its value at equilibrium, then the spreading time is proportional to the square of the degree of polymerization and inversely proportional

to the fifth power of the starvation factor:

$$\tau_s = \tau_0 f N^2 x^{-5} \tag{21}$$

If saturation is achieved, then the starvation factor, x, equals $N^{-1/5}$. Substituting into eq 21, we see that the spreading time is proportional to the third power of the degree of polymerization, $\tau_s \propto \tau_0 f N^3$, indicating a reptation process in the vicinity of the wall, with a higher friction.

From the above it is evident that to determine the rate limiting process we must compare the time for entry to the time for spreading. Entry will be the rate controlling step if the wall friction coefficient, f, is less than $Nx^{3.5}$. In this case the rate of adsorption equals the net rate of entry of new chains into the already existing layer. Under the assumption that the exit rate of chains from the layer is negligible, it is shown (27) that the net rate of entry is proportional to the solution concentration and inversely proportional to the entry time, τ_e:

$$\frac{d\Gamma}{dt} = \frac{c_b}{c^*}\frac{1}{R_F^2}\frac{1}{\tau_e} \tag{22}$$

Substituting the expression for the entry time (equation 20) and transmission coefficient ϑ, we have a differential equation that describes the rate of adsorption as a function of degree of polymerization, bulk solution concentration, and the microscopic jump time:

$$-\Gamma_0\frac{dx}{dt} = \frac{c_b}{c^*}\frac{1}{R_F^2}\frac{x^{3/2}}{\tau_0 N^3} \tag{23}$$

The above equation can be solved analytically, with the initial condition of a completely starved layer, $x = 1$ for $t = 0$, resulting in the following expression of the surface excess (adsorbed amount) as a function of time:

$$x = \left(\frac{2\theta}{t+2\theta}\right)^2 \quad \text{with } \theta = \frac{c^* R_F^2 \tau_0 N^3 \Gamma_0}{c_b} \tag{24}$$

Displacement experiments by Tassin[18] and Peffekorn[14-17] have shown that the polymer chains in the adsorbed layer will exchange at a finite rate with the chains in the solution. Similarly, they have shown that the adsorbed polymer layer will not dissolve when the layer is brought in contact with pure solvent. A similar observation was made in this study when the adsorbed polystyrene layer was brought in contact with pure carbon tetrachloride. Granick[21] has shown that an already weakly adsorbed polymer will not be readily displaced by a more strongly adsorbing polymer because of steric barriers. These observations indicate that the rate of desorption of an already existing layer is almost negligible. On the other hand, the exchange rate of the adsorbed polymer chains might have a finite value.

It is interesting to note that for concentrations in the entanglement regime the solution and the adsorbed layer behave like meshes with different sizes. Thus, the change of chemical potential due to adsorption, $\Delta\mu$, per monomer should follow the same scaling as the difference in chemical potentials between solutions of different mesh sizes, one with a mesh size equal to the Flory radius, R_F, corresponding to the solution and one with a size equal to the thickness of the adsorbed layer, l[27]

$$\Delta\mu \approx kT\left(\frac{1}{g(l)} - \frac{1}{N}\right) \underset{N\to\infty}{\rightarrow} \frac{kT}{g(l)} \approx kTx^{-5} \tag{25}$$

For a saturated layer the starvation coefficient is equal to $N^{-1/5}$; thus the chemical potential gain for a saturated layer is equal to NkT. For large N the adsorption energy per chain becomes very large, even if the adsorption energy per segment is small. This is an interesting result because it explains the very strong attraction of the polymer chains to the solid surface. As the layer becomes saturated ($x \rightarrow 0$), the chemical potential change, due to adsorption, becomes larger, indicating a stronger binding of the polymer chains at the solid surface. This observation suggests that only for highly starved layers ($x \rightarrow 1$) will the macromolecular chain encounter competition for which environment it will reside in, solution or adsorbed layer.

de Gennes[26] has shown that if exchange between the adsorbed layer and the solution is significant, then its rate will also be limited by the ability of the chain to exit the adsorbed layer. Thus, the rate of exchange will be inversely proportional to the entry time and proportional to the amount of polymer adsorbed:

$$-\frac{d\Gamma}{dt} = \frac{\Gamma}{N}\frac{1}{\tau_e}\exp\left(\frac{\Delta\mu}{kT}\right) \tag{26}$$

The exponential term ensures detailed balance, because of the difference in chemical potential of a monomer in solution and in the adsorbed layer. Substituting eq 25 gives

$$-\frac{d\Gamma}{dt} = \frac{\Gamma}{N}\frac{1}{\tau_e}\exp(x^{-5}) \tag{27}$$

Equations 23 and 27 can be combined to yield an expression for the net rate of adsorption:

$$\frac{dx}{dt} = -\frac{c_b}{c^*}\frac{1}{R_F^2}\frac{x^{3/2}}{\tau_0 N^3 \Gamma_0} + \frac{1-x}{\tau_0 N^4}x^{3/2}\exp(x^{-5}) \tag{28}$$

This equation can be solved numerically to provide the starvation factor as a function of time.

Comparison between the Theoretical Model and Experimental Results

Assuming no exchange, as explained above, one can use eq 24 to fit the experimental results. There is only one adjustable parameter, θ, from which the experimental microscopic jump time, τ_0, can be calculated. The predicted starvation coefficient is compared to the experimental data in Figure 8. It is seen from these figures that the model predictions and the experimental data agree rather well. The value also of the microscopic jump time calculated from the regression is in the picosecond range. The theoretical value of the microscopic jump time is calculated from eqs 14–16. The two values of τ_0 are shown in Table 3. The theoretically predicted and experimentally calculated values of τ_0, as shown in Table 3, follow the same trend with respect to concentration and molecular weight. The last column of the table exhibits the ratio of the two values and can be interpreted as the additional friction encountered by the incoming polymer chain, because of the constrained state of the initially adsorbed macromolecules. de Gennes names this friction coefficient the glassy friction coefficient. It must be noted, however, that there is no glassy state present, simply the adsorbed molecules exhibit a greater constraint because of the presence of the surface. It is easily seen that f has a smaller value for the samples for which the rate of adsorption is greater. With increasing solution concentrations the adsorbed layer becomes more fluidlike, indicative of the

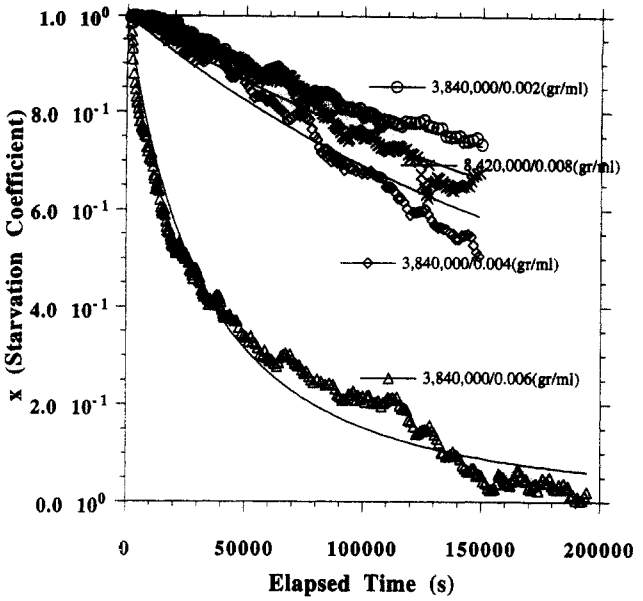

Figure 8. Starvation coefficient as a function of time, for four different samples. The solid line represents the model prediction, and the points are the experimentally determined starvation coefficients.

Table 3. Summary of Predicted and Experimentally Determined Microscopic Jump Times

MW	c (g/mL)	c_e (g/mL)	R_F (Å)	Γ_0 (g/cm^2)	τ_0^e (ps)	τ_0^{th} (ps)	f
3 840 000	0.002	0.007	600	1×10^{-6}	4.25	0.80	5.3
3 840 000	0.004	0.007	600	1×10^{-6}	4.70	0.84	5.6
3 840 000	0.006	0.007	600	1×10^{-6}	0.93	0.68	1.4
8 420 000	0.008	0.0048	888.5	1×10^{-6}	1.75	0.74	2.4

decreasing f value. With increasing molecular weight it is well established[4] that the fraction of segments in trains decreases, while the fraction of segments in tails increases, thus making the adsorbed layer more fluidlike. This is evident, again, from the predicted f value. For the 8 420 000 molecular weight sample the glassy friction coeffiicient is less than the corresponding coefficient for the 3 840 000 samples for similar surface coverages. These observations are in accordance with the physical model used to interpret the behavior of the experimental results. Additionally, the reptational character of the entry process also explains the slower rate of adsorption with increasing molecular weight. As already discussed, the entry time scales with N^3. For the samples of concentration 0.008 g/mL and molecular weights of 3 840 000 and 20 600 000, the model with no desorption does not work well.

The two stage adsorption behavior observed for the 0.008 g/mL concentration of the MW = 3 840 000 sample and 0.0178 g/mL concentration of the MW = 600 000 sample can be explained through a two stage mechanism. The initial stage involves establishing an equilibrium between the exchange of macromolecular chains at the initially adsorbed material–solution interface, as discussed in the previous section. Once equilibrium is established at the interface, polymer chains diffuse via reptation to the solid–polymer interface where adsorption takes place. This two stage mechanism has been found[46] to work also very well for non-Fickian diffusion of solvent vapor into glassy polymers. The diffusion of the polymer chains through the adsorbed layer is a process that can be simulated by a simple penetration equation with a first order reversible reaction taking place at the solid–liquid interface

$$\frac{\partial c}{\partial t} = D\frac{\partial^2 c}{\partial x^2} \tag{29}$$

with the following initial and boundary conditions:

$$t = 0:\ c = c_0 \tag{30}$$

$$\text{at } x = 0:\ \frac{d\Gamma}{dt} = -D\frac{\partial^2 c}{\partial x^2}\bigg|_{x=0} = kc(t,0)\left(\Gamma_m - \frac{\Gamma}{k_d}\right) \tag{31}$$

$$\text{at } x = l:\ V\frac{\partial c}{\partial t} = -AD\frac{\partial c}{\partial x}\bigg|_{x=l} \tag{32}$$

Where V is the volume and A is the cross sectional area. The above model can be solved using Laplace transforms, and the solution is presented in Appendix A. As discussed earlier, for this solution concentration, near the entanglement concentration, the exchange rate is important. Solving eq 29 numerically and plotting the starvation coefficient as a function of time, shown in Figure 9, we get an acceptable agreement between the theoretical model and the experimental data for the first plateau. According to this model, the duration of the first plateau will decrease with the increasing diffusion coefficient of the penetrating polymer molecule. This effect is observed when the 0.008/3 840 000 and 0.0178/600 000 samples are compared. For the high molecular weight sample, the duration of the first plateau is approximately 15 h, and for the lower molecular weight it is approximately 4 h. The diffusion coefficient of the entering molecule increases with decreasing molecular weight; thus diffusion of the smaller molecule is faster.

The second plateau can be simulated by the model described earlier. Unfortunately, predicting values for the kinetic coefficients is not possible and thus no attempt to model the second plateau was attempted.

Conclusions

Experimental results concerning the adsorption of narrow molecular weight polystyrene on germanium from its carbon tetrachloride solution are presented. We have shown the applicability of attenuated total reflection spectroscopy for measuring the adsorption kinetics *in situ*. Expanding upon the model first proposed by de Gennes, we have identified the rate limiting step to be the entry process in the immediately established polymer layer. This constrained layer offers an increasing degree of resistance as the fraction of adsorbed segments increases. Additionally, we have postulated a two stage mechanism that explains the step kinetics observed in our experimental results as well as in data of other researchers.

When comparing the experimental observations of our system with the typically studied systems of a small degree of polymerization macromolecules, and low concentration solution samples, we observe very slow kinetics, caused by the reptational nature of the rate limiting step. The experimental data also suggest the presence of nonequilibrium states that are caused by the slow reptational motion of very large molecules. The suggested model predicts microscopic jump times that are in good agreement with the theoretically predicted values.

Appendix A

One-dimensional non-steady-state diffusion is described by

$$\frac{\partial c}{\partial t} = D\frac{\partial^2 c}{\partial x^2} \tag{A.1}$$

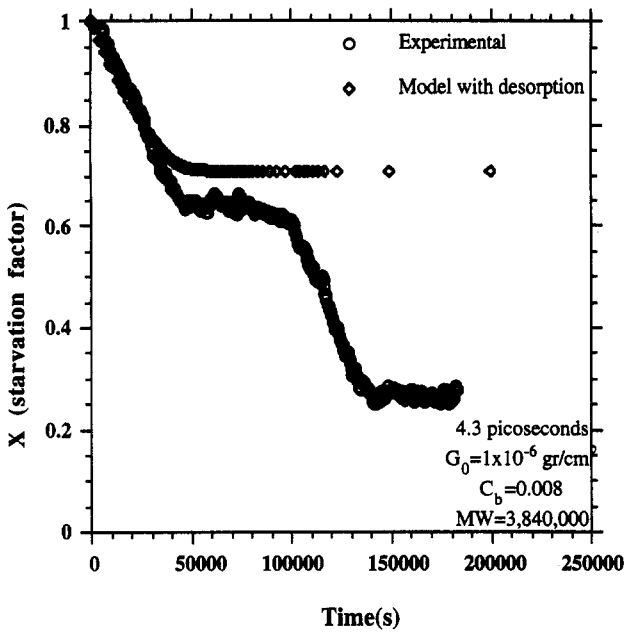

Figure 9. Starvation coefficient as a function of time, for the 3 840 000 molecular weight sample with a solution concentration of 0.008 g/mL. The diamonds (upper curve) represent the model prediction, and the circles are the experimentally determined starvation coefficients.

The uniform initial condition is used

$$t = 0 \rightarrow c = c_0$$

as well as the following boundary conditions:

$$x = 0 \rightarrow d\left.\frac{\partial c}{\partial x}\right|_{x=0} = k_a\left(\Gamma_m c(0,t) - \frac{\Gamma}{K_a}\right) = \frac{d\Gamma}{dt} \quad \text{(A.2)}$$

$$x = l \rightarrow \frac{V}{A}\left.\frac{\partial c}{\partial t}\right|_{x=l} = \left.\left(-D\frac{\partial c}{\partial x}\right)\right|_{x=l} \quad \text{(A.3)}$$

We dedimensionalize the variables as follows:

$$c' = \frac{c}{c_0} \qquad x' = \frac{x}{L} \qquad \eta = \frac{1}{L} \qquad \tau = \frac{Dt}{L^2} \qquad \theta = \frac{\Gamma}{\Gamma_m}$$

Substituting into eq A.1

$$\frac{\partial c'}{\partial t} = \frac{\partial^2 c'}{\partial x'^2} \quad \text{(A.4)}$$

The initial and boundary conditions become

$$\tau = 0 \rightarrow c' = 1 \quad \text{(A.5)}$$

$$x' = 0 \rightarrow \xi\frac{d\theta}{dt} = \frac{\partial c'}{\partial x'} = \Phi[c'(0,\tau) - \epsilon\theta] \quad \text{(A.6)}$$

$$x' \rightarrow \eta \rightarrow \frac{\partial c'}{\partial \tau} = -\frac{\partial c'}{\partial x'} \quad \text{(A.7)}$$

with

$$\Phi = \frac{k_a c_0 L^2}{D} \qquad \epsilon = \frac{1}{K_a c_0} \qquad \xi = \frac{\Gamma_m}{L c_0}$$

The characteristic length, L, can be any characteristic dimension in the geometry of the system. In this case the thickness of the adsorbed layer is used, so $\eta = 1$ for the system under consideration.

The partial differential equation described by eqs A.4–A.7 can be solved analytically using the Laplace transforms technique.[47-48] The Laplace transformation of the concentration profile is given by

$$\bar{c}(x,s) = \frac{c_0}{2} - c_0\{(\Phi\xi\sqrt{s})\sinh[\sqrt{s}(\eta - x)] + (\Phi\xi)\cosh[\sqrt{s}(\eta - x)]\}/\left\{(s^2 + \Phi\epsilon s + \Phi\xi s)\cosh(\eta\sqrt{s}) + (s^2 + \Phi\epsilon s + \Phi\xi s^2)\frac{\sinh(\eta\sqrt{s})}{\sqrt{s}}\right\} \quad \text{(A.8)}$$

Inversion of this Laplace transformation is done using the Laplace inversion theorem, and integration, using the method of residuals.[47] This results in the following concentration profile:

$$c(x,t) = \frac{c_0\epsilon}{\epsilon + \xi} - \sum_{k=1}^{\infty}\frac{\Phi_1(x,s_k)\exp(s_k\tau)}{\Phi_2(s_k)} \quad \text{(A.9)}$$

s_k are the roots of the denominator of the right hand side of eq A.8, and its values are always negative. Φ_1 and Φ'_2 are calculated as follows:

$$\Phi_1(x,s_k) = \frac{\eta}{2\sqrt{s_k}}\sinh(\eta\sqrt{s_k})(s_k^2 + \Phi\epsilon s_k + \Phi\xi s_k) + \cosh(\eta\sqrt{s_k}) \quad \text{(A.10)}$$

$$\Phi'_2(s_k) = \cosh(\eta\sqrt{s_k})\left[2s_k\Phi\epsilon + \Phi\xi + \frac{\eta}{2}(s_k + \Phi\epsilon + \Phi\xi s_k)\right] + \frac{\sinh(\eta\sqrt{s_k})}{\sqrt{s_k}}\left[\frac{\eta}{2}(s_k^2 + \Phi\epsilon s_k + \Phi\xi s_k)\right] + \frac{1}{2}(3s_k + \Phi\epsilon + 3\Phi\xi s_k) \quad \text{(A.11)}$$

From the above expression of the concentration profile the surface coverage can be evaluated as well,[49] using eq A.6:

$$\theta(\tau) = \frac{c_0\epsilon}{\epsilon+\xi}(1 - \exp[-\epsilon\Phi\tau]) - \Phi\sum_{k=1}^{\infty}\frac{\Phi_1(0,s_k)(\exp[s_k\tau] - \exp[-\epsilon\Phi\tau])}{(-s_k)(\epsilon\Phi + s_k)\Phi'_2(s_k)} \quad \text{(A.12)}$$

Nomenclature

$\langle s^2\rangle^{1/2}$	radius of gyration (Å)
A	integrated absorption
α	absorption coefficient
a	monomer size (Å)
C	polymer concentration in solution (g/mL)
C^*	overlap concentration (g/mL)
C_b	bulk solution concentration
C_i	interfacial concentration
D	diffusion coefficient
d_e	effective thickness
d_p	penetration depth
ϵ	molecular emmisivity
E_0	electric field amplitude at the interface, in the rarer medium
E_{oi}	electric field amplitude at the interface, in the i-direction
f	glassy friction coefficient

ϕ	volume fraction of polymer
Γ	surface excess, monomers per unit area
Γ_0	maximum surface excess
Γ_i	surface excess
η	refractive index
ν	solution viscosity (P)
η_{21}	ratio of the refractive indices of the rarer and denser medium
ν_s	solvent viscosity (P)
ϑ	tunneling barrier coefficient
φ	angle of refraction
k	Boltzmann coefficient
l	thickness of the adsorbed layer (Å)
λ	wavelength (μm)
N	degree of polymerization
N_r	number of reflections
N_A	Avogadro number (6.023×10^{23} molecules/mol)
θ	angle of incidence
R	reflectivity
R_F	Flory radius (Å)
R_h	hydrodynamic radius (Å)
T	temperature (K)
τ_0	microscopic jump time (ps)
τ_e	entry time (s)
τ_s	spreading time
ξ	correlation length of a polymer solution
x	starvation coefficient
ζ_G	solvent–monomer friction coefficient in glassy conditions
ζ_s	solvent–monomer friction coefficient
μ	chemical potential
V	volume
z	direction in which the Ir radiation is penetrating

References and Notes

(1) Cohen Stuart, M. A.; Cosgrove, T.; Vincent, B. *Adv. Colloid Interface Sci.* **1986**, *24*, 143.
(2) de Gennes, P. G. *Adv. Colloid Interface Sci.* **1987**, *27*, 189.
(3) Takahashi, A.; Kawagushi, M. *Adv. Polym. Sci.* **1982**, *46*, 1.
(4) Kawagushi, M.; Hayakawa, K.; Takahashi, M. *Macromolecules* **1983**, *16*, 631.
(5) Kawagushi, M.; Takahashi, A. *J. Polym. Sci., Polym. Phys. Ed.* **1980**, *18*, 2069.
(6) Kawagushi, M.; Takahashi, A. *Macromolecules* **1983**, *16*, 1465.
(7) Takahashi, A.; Kawagushi, M.; Hirota, H.; Kato T. *Macromolecules* **1980**, *13*, 884.
(8) Priel, Z.; Silerberg, A. *J. Polym. Sci., Polym. Phys. Ed.* **1978**, *16*, 1917.
(9) Varoqui, R.; Dejardin, P. J. *Chem. Phys.* **1977**, *66*, 4395.
(10) Barnet, K. G.; et al. *Macromolecules* **1981**, *14*, 1018.
(11) Barnet, K. G.; et al. *Polymer* **1981**, *22*, 283.
(12) Day, J. C.; Robb, D. I. *Polymer* **1980**, *21*, 408.
(13) Kawagushi, M.; Hayakawa, K.; Takahashi, A. *Polym. J.* **1980**, *12* (4), 265.
(14) Peffekorn, E.; Carroy, A.; Varoqui, R. *Macromolecules* **1985**, *18*, 2252.
(15) Peffekorn, E.; Carroy, A.; Varoqui, R. *J. Polym. Sci., Polym. Phys. Ed.* **1985**, *23*, 1997.
(16) Peffekorn, E.; Haouam, A.; Varoqui, R. *Macromolecules* **1988**, *21*, 2111.
(17) Peffekorn, E.; Haouam, A.; Varoqui, R. *Macromolecules* **1989**, *22*, 2677.
(18) Tassin, J. F.; Siemens, R. L.; et al. *J. Phys. Chem.* **1989**, *93*, 2106.
(19) Zhang, Y.; Levy, Y.; Loulergue, J. C. *Surf. Sci.* **1987**, *184*, 214.
(20) Frantz, P.; Granick, S. *Phys. Rev. Lett.* **1991**, *66*, 899.
(21) Johnson, H. E.; Granick, S. *Science* **1992**, *255*, 966.
(22) Kuzmenka, D. J.; Granick, S. *Colloids Surf.* **1988**, *31*, 105.
(23) McKeigue, K.; Gulari, E. *Surfactants Solution* **1984**, *2*, 1271.
(24) Peyser, P.; Stromberg, R. R. *J. Phys. Chem.* **1967**, *71*, 2066.
(25) van der Beek, G. P.; Cohen Stuart, M. A.; Fleer, G. J. *Macromolecules* **1991**, *24*, 3553.
(26) de Gennes, P. G. *C. R. Acad. Sci., Ser. 2* **1985**, *301*, 1399.
(27) de Gennes, P. G. In *New Trends in Physics and Physical Chemistry of Polymers*; Lieng-Huang Lee, Ed.; Plenum Press: New York, 1989.
(28) Harrick, N. J. *Internal Reflection Spectroscopy*; Interscience Publishers John Wiley & Sons: New York, 1967.
(29) Iwamoto, R.; Ohta, K. *Appl. Spectrosc.* **1984**, *38*, 359.
(30) Ohta, K.; Iwamoto, R. *Appl. Spectrosc.* **1985**, *39*, 418.
(31) Ohta, K.; Iwamoto, R. *Anal. Chem.* **1985**, *57*, 2491.
(32) Tompkins, H. G. *Appl. Spectrosc.* **1974**, *28*, 335.
(33) Sperline, R. P.; Muralidharan, S.; Freiser, H. *Appl. Spectrosc.* **1986**, *40*, 1019.
(34) Sperline, R. P.; Muralidharan, S.; Freiser, H. *Langmuir* **1987**, *3*, 198.
(35) Sperline, R. P.; Freiser, H. *Langmuir* **1990**, *6*, 344.
(36) Sperline, R. P. *Appl. Spectrosc.* **1991**, *45*, 677.
(37) Onishi, T.; Krimm, S. *J. Appl. Phys.* **1961**, *32*, 2320.
(38) Painter P. C.; Koenig, J. L. *J. Polym. Sci.* **1977**, *15*, 1885.
(39) Auvray, L.; Cotton, J. P. *Macromolecules* **1987**, *20*, 202.
(40) de Gennes, P. G. *Scaling Concepts in Polymer Physics*, Cornell University Press, Ithaka, 1979.
(41) Doi, M.; Edwards, *J. Chem. Soc., Faraday Trans. 2* **1978**, *74*, 1789, 1802, 1818.
(42) Kirkwood, J. G.; Baldwin, R. L.; Dunlop, P. J.; Gosting, L. J.; Kegeles, G. *J. Chem. Phys.* **1960**, *33*, 1505.
(43) Elaaissari, A.; Haouam, A.; Huguenard, C.; Peffekorn, E. *J. Colloid Interface Sci.* **1992**, *149*, 68.
(44) Cohen Stuart, A.; Tamai, H. *Colloids Surf.* **1988**, *31*, 265.
(45) Cohen Stuart, A.; Tamai, H. *Macromolecules* **1988**, *21*, 1863.
(46) Bagley, E.; Long, F. A. *J. Am. Chem. Soc.* **1955**, *77*, 2172.
(47) Kreyszig, E. *Advance Engineering Mathematics*, 6th ed., John Wiley & Sons: New York, 1988.
(48) Jenson, V. G.; Jeffreys, G. V. *Mathematical Methods in Chemical Engineering*, 2nd ed.; Academic Press: London, 1977.
(49) Melik, D. H. *J. Colloid Interface Sci.* **1990**, *138*, 397.